ISSN 1225-8024(Print)
ISSN 2288-8403(Online)
<연구논문>

한국표면공학회지
J. Korean Inst. Surf. Eng.
Vol. 49, No. 2, 2016.
http://dx.doi.org/10.5695/JKISE.2016.49.2.152

Effects of Plasma Treatment on Contact Resistance and Sheet Resistance of Graphene FET

Chang-Ho Ra, Min Sup Choi, Daeyeong Lee, and Won Jong Yoo*

SKKU Advanced Institute of Nano-Technology (SAINT), Samsung-SKKU Graphene Center (SSGC),
Sungkyunkwan University, 2066 Seobu-ro, Jangan-gu, Suwon 16419, Korea

(Received February 27, 2016 ; revised April 6, 2016 ; accepted April 27, 2016)

Abstract

We investigated the effect of capacitively coupled Ar plasma treatment on contact resistance (R_c) and channel sheet resistance (R_{sh}) of graphene field effect transistors (FETs), by varying their channel length in the wide range from 200 nm to 50 μm which formed the transfer length method (TLM) patterns. When the Ar plasma treatment was performed on the long channel (10 ~ 50 μm) graphene FETs for 20 s, R_c decreased from 2.4 to 1.15 kΩ·μm. It is understood that this improvement in R_c is attributed to the formation of sp^3 bonds and dangling bonds by the plasma. However, when the channel length of the FETs decreased down to 200 nm, the drain current (I_d) decreased upon the plasma treatment because of the significant increase of channel R_{sh} which was attributed to the atomic structural disorder induced by the plasma across the transfer length at the edge of the channel region. This study suggests a practical guideline to reduce R_c using various plasma treatments for the R_c sensitive graphene and other 2D material devices, where R_c is traded off with R_{sh}.

Keywords : Graphene, Plasma, Contact resistance, Sheet resistance, Field effect transistor

1. Introduction

In recent years, graphene has been studied intensively because of its high mobility, transparent, flexible and excellent thermal properties [1,2]. However, the performances of graphene device are still limited seriously by the factors such as defects, impurities, and R_c. In particular, R_c should be reduced significantly for practical application. Parrish *et al.* reported quantitatively that the increase of R_c affects largely the key performances of the graphene FETs including the current density, trans-conductance, self-gain and transit-frequency [3]. It is understood that R_c of graphene devices is caused by two factors. The one is residues, such as PMMA and PR generated during photolithography and transfer processing, and the other is coherence at the junction between metal and graphene.

There have been various studies to reduce R_c by controlling these factors. It is reported that R_c of graphene devices generated by residues could be reduced by O_2 plasma cleaning followed by annealing [4,5], introduction of Al_2O_3 passivation layer [6], UV O_3 treatment [7,8], Ar plasma treatment [9,10], CO_2 cluster treatment [11], X-ray [12] and O_2 plasma [13]. Nagashio *et al.* reported about coherence between Ti, Cr, Ni and graphene which is also one of the key parameters for inducing R_c [14-16]. In this regard, other groups reported mechanisms on the generation of R_c at the interface between metal and 2D materials using a carrier transport model [17], a tunneling model [18] and also demonstrated the reduction of R_c using a metal/graphene/metal sandwiched structure [19]. Meanwhile, the studies to reduce R_c by forming the edge contact has recently been studied. The simulation results firstly suggested the superiority of edge contact to side contact [20] and they were then verified experimentally by using patterned graphene,

*Corresponding Author: Won Jong Yoo
Sungkyunkwan University
Tel: +82-31-290-7468 ; Fax: +82-31-299-4119
E-mail: yoowj@skku.edu

h-BN/Gr/h-BN 1-D contact structure and Ni-etched graphene contact [21-23].

Among these, plasma treatment can be the most desirable method to improve R_c for the large area graphene devices since it is readily adopted from the conventional electronic device fabrication processing with the advantage of low temperature and large-scale processing over other contending techniques. However, the plasma treatment can induce significant damage onto graphene and therefore decrease electrical performance of devices, due to the ion bombardment generated by highly ionized plasma. But if a special graphene structure to avoid energetic ion bombardment is used to decrease R_c, the electrical performance of graphene devices can be improved. Chen *et al.* reported to design a modified graphene structure with vacancies generated by Ar plasma treatment [24], and R_c of graphene device was expected to be reduced by using this modified graphene structure. In this study, we demonstrated the effects of Ar plasma treatment on R_c and R_{sh} of modified graphene structure devices with various scaling ranges from micro- to nano-scale channel length. This study gives the insight for pros and cons of plasma-treated graphene and other 2D material based devices.

2. Results and Discussion

The graphene film grown on Cu foil by CVD method was used for this study. The Cu foil was introduced into a glass chamber in which temperature increased up to 1000 °C with flowing H_2 of 10 sccm. Then, heat treatment was carried out for 15 min and CH_4 of 50 sccm was additionally introduced. The graphene film was grown on the Cu foil via crystallization during cooling for 30 min. The PMMA was deposited to protect the graphene. The graphene was floated for 6 hr in 10 g of ammonium persulfate solution dissolved in 0.5 l of DI water to remove the Cu foil. The graphene was subsequently transferred onto a 90 nm thick silicon oxide substrate. Then, it was rinsed in DI water and the PMMA was removed with acetone [25,26].

The Ar plasma discharged at 6 W power with 0, 10, 20 and 30 s treatment times was used in this study. Fig. 1(a) displays the contact angles depending on plasma treatment times. It was observed that the contact angle decreased from 87 to 7.2 degrees with increasing plasma treatment time. The contact angle results show that the graphene was transformed from hydrophobic to hydrophilic by the plasma treatment. We understand that the adhesion of metal is improved when graphene becomes more hydrophilic. This implies the possibility to improve the contact properties between graphene and metals as reported previously [10], where the scaling effects on R_c and R_{sh} of plasma-treated graphene devices, however, wasn't investigated.

Figure 1(b) displays the Raman data of the treated

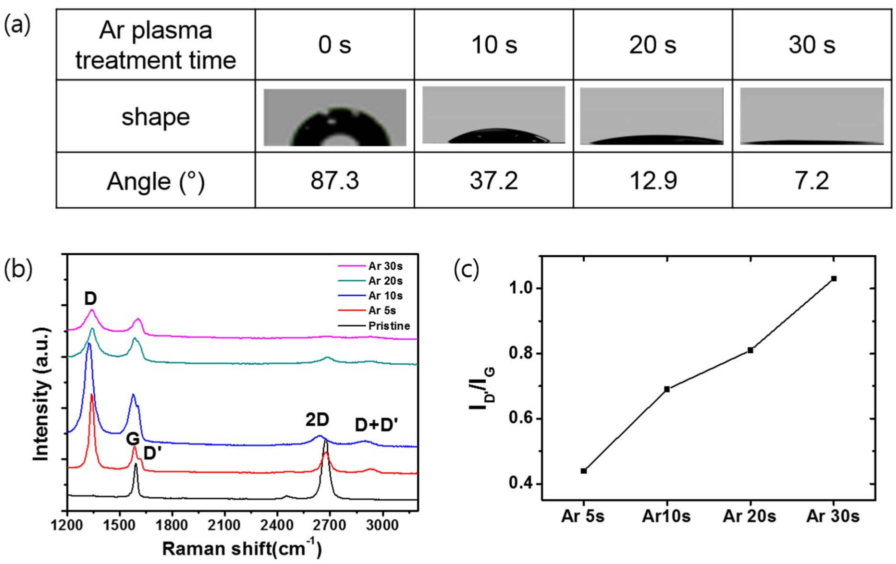

Fig. 1. (a) Contact angles for different plasma treating times. The graphene property was changed from hydrophobic to hydrophilic by Ar plasma treatment. (b) Raman spectra of the pristine and plasma treated graphene films. D' peak is generated by Ar plasma treatment at 6 W, indicating the generation of graphene vacancies. (c) Intensity ratio of D' peak to G peak, depending on plasma treating time.

devices. The Raman data showed the D' and D'+D peaks at 1623 cm^{-1} and 2939 cm^{-1}, respectively. D peak is related to sp^2 bonding [27,28]. But D' peak is known to be more closely related to the generation of vacancies than defects [29,30]. When the Ar inductively coupled plasma (ICP) treatment was conducted instead of Ar capacitively coupled plasma (CCP), D' peak was not generated. It was found that the D' and D'+D peak intensities increased with increasing plasma treatment time. In particular, the ratio of $I_{D'}/I_G$ was 0.69 for the case of 10 s plasma treatment and increased to 1.03 for 30 s as shown in Fig. 1(c). It suggests the generation of vacancies which could help to lower R_c by inducing the edge contact with metal as previously reported [20,21,24].

Figure 2(a) shows the device fabrication sequence including Ar plasma treatment. R_c was measured by using the transfer length method (TLM). After patterning process (photo-lithography for long channel devices and electron beam lithography short channel devices), the Ar CCP with power of 6 W was applied to graphene prior to deposition of electrodes. That is, The Ar plasma treatment was conducted before metal deposition to change the surface property of metal contact region of graphene. This was to protect the graphene as the FET channel from being damaged by the ion bombardment of the plasma. Cleaning of graphene by low power ICP treatment was reported [9], in which graphene was however damaged after the extended treatment exceeding optimized duration because graphene channel region is directly exposed by plasma. In contrast, the graphene channel can be protected against plasma due to the covered polymers such as PR or PMMA for our devices. After plasma treatment, 20/40 nm thick Pd/Au electrodes were deposited by electron beam evaporation. The evaporated electrodes were lifted off by acetone. Fig. 2(b) shows an optical microscopic image of a fabricated plasma-treated graphene device with short channel lengths. The width of the device is 25 μm and the lengths are 10 ~ 50 μm for the long channel, and width is 1.2 μm and lengths are 200 nm~1 μm for the short channel devices.

Figure 3(a) shows the electrical properties measured at V_G-V_{Dirac} = –30 V for a TLM device treated by Ar plasma at 6 W for 10, 20 and 30 s, where V_{Dirac} is the voltage at Dirac point. The total resistance (R_{tot}) is obtained from the I_d-V_d results obtained in the range of V_d = –0.01 ~ 0.01 V. TLM equation can be expressed as

$$R_{tot} = R_{sh}\frac{L}{W} + 2R_c$$

where R_{sh} is the sheet resistance, L is the channel length and W is the channel width. According to this equation, the slope in the R_{tot} vs L curve becomes R_{sh}/W and the y-intercept becomes $2R_c$ as shown in Fig. 3(e). It shows that the total resistance was lowered when the Ar 6W CCP treatment was carried out for 10 and 20 s, and then increased for 30 s. The R_c was estimated by multiplying each y-intercept of Fig. 3(a) to W of 25 μm. As shown in Fig. 3(b), the values of 2.4, 2.1, 1.15, and 2.4 kΩ·μm were calculated for the pristine, 10, 20 and 30 s treated devices, respectively. The R_c becomes the lowest value when 6 W Ar CCP treatment is conducted for 20 s.

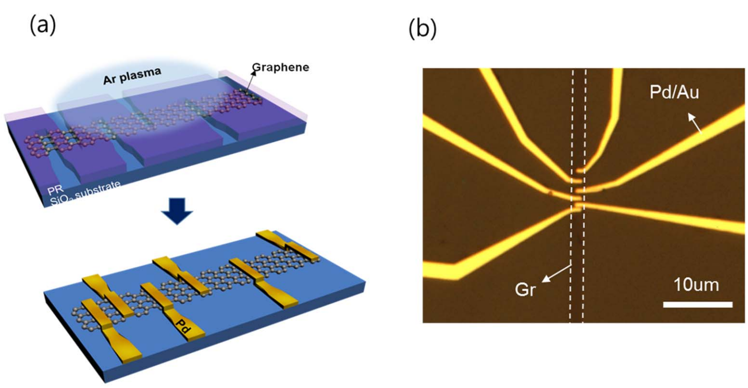

Fig. 2. (a) Fabrication process of a plasma treated graphene device. Graphene channel is protected by PR during plasma treatment. Ar plasma treatment is performed on graphene on which metal is deposited subsequently. (b) Optical microscopic image of TLM patterns with 20/40 nm thick Pd/Au electrodes for short channel device. The channel width is 25 μm and lengths are 10 ~ 50 μm for long channel device, and width is 1.2 μm and lengths are 200 nm ~ 1 μm for short channel device.

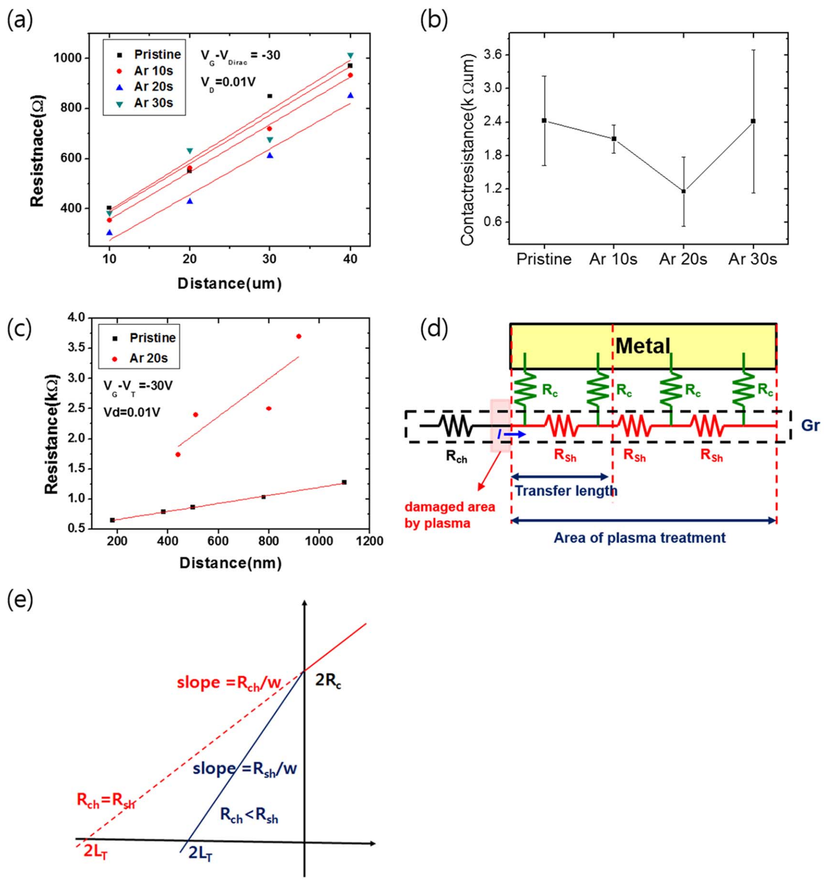

Fig. 3. (a) TLM results for the devices treated by Ar plasma for 0, 10, 20 and 30 s at V_g-V_{Dirac} = - 30 V. (b) R_c of pristine and plasma treated graphene devices. R_c is 1.15 kΩ·um for the device plasma treated at 6 W for 20 s. (c) TLM results for the devices treated by Ar plasma for 0 and 20 s for short channel device. (d) Electric circuit involving metal/graphene contact which shows that L_T region could be affected by plasma treatment since it is not protected from Ar ion bombardment. (e) Schematic model showing the relationship between L_T and R_{sh}. The y-intercept is $2R_c$ and linear slope represents R_{sh} according to the TLM fitting.

The reason for such a low R_c was thought to originate from the same effects as the formation of edge contacts and the generation of sp^3 bonding in the vacancy by the Ar plasma [24]. This is because the 20 s Ar plasma treatment lowered the total resistance of the device. However, the 10 s treatment showed only a marginal reduction because the creation of the vacancies and the resultant sp^3 bonding were probably insufficient. The increased R_c at 30 s seems to be attributed to the excessive surface damage by Ar plasma. Although R_c is significantly changed by plasma treatments, the extracted R_{sh} values from Fig. 3(a) through TLM equation are similar, in the range of 455 ~ 500 Ω/□ before and after 20 s plasma treatment because the graphene channel was protected by the PR, as described in Fig. 2(a). Thus, the effects of plasma on graphene channel region could be ignored for long channel devices.

Figure 3(c) shows TLM results of before and after 20 s Ar plasma treatment for the short channel devices. R_c of the pristine device is 527 Ω·μm, whereas that of the 20 s plasma treated device is 494 Ω·μm. Although the R_c is just slightly decreased compared to the long channel device, the extracted R_{sh} (3.13 kΩ/□) of 20 s Ar plasma treated device is much higher than that (0.67 kΩ/□) of pristine device. In order to explain these differences between long and short channel devices, we suggest a schematic electric circuit model involving the metal/graphene contact at DC voltage as shown in Fig. 3(d). By applying KVL (Kirchhoff's voltage law) and KCL (Kirchhoff's current law) into this circuit, the following relationship between R_c and R_{sh} can be expressed as

$$R_c = \frac{R_{sh}}{W} L_T$$

where L_T is the transfer length. The details to obtain this equation are shown in Supporting Information: Relationship between R_c and L_T.

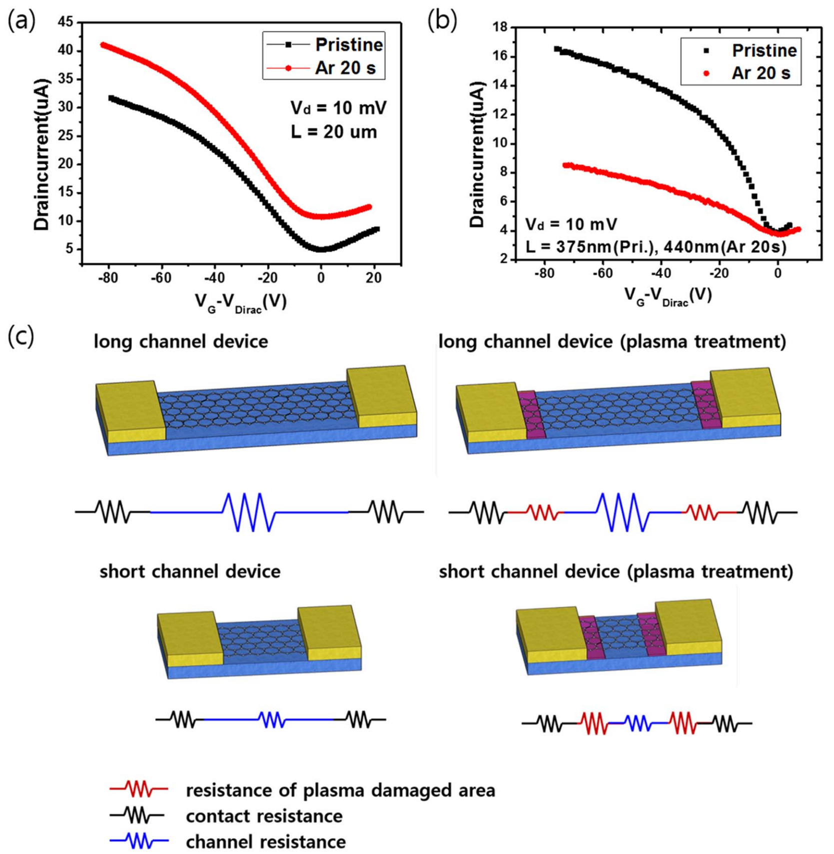

Fig. 4. I_d-V_g at V_d = 10 mV for (a) long channel device and (b) for short channel devices. (c) Schematic diagrams comparing long channel and short channel devices without and with plasma treatment.

Meanwhile, Fig. 3(e) shows that the intercept of x-axis becomes $2L_T$ from the TLM equation [17, 31-33]. However, the slope of straight line is shifted to the positive direction by plasma treatment, which indicates the decrease of L_T. The corresponding L_T becomes 616, 302 and 463 nm for 10, 20 and 30 s, respectively. According to the equation on relationship between R_c and R_{sh}, the R_c is proportional to the R_{sh} and L_T. Thus, if the L_T is decreased and R_{sh} is maintained after plasma treatment, R_c could be reduced. For the long channel devices, this analysis is consistent with our obtained electrical properties since R_{sh} is unchanged after plasma treatment as mentioned previously. As a result, the decreased L_T and unchanged R_{sh} result in reduction of R_c. For the short channel device, however, R_{sh} could be higher after plasma treatment. This is because the damaged region extended into the channel induced by the plasma treatment, which is close to the contact region, can be relatively larger than that of the long channel device. The damaged region in the channel is described in Fig. 3(d). It has been reported that O_2 plasma could etch graphene in horizontal direction with increasing treatment time [13]. Although Ar plasma is anisotropic, the increased treatment time can give rise to the damaged region in the channel. In order to verify our analysis, we compared R_{sh} before and after plasma treatment, for both cases of plain graphene (without undergoing device processing) and short channel TLM device processed graphene. The measured R_{sh} values from the plain graphene are 0.4 and 3.8 kΩ/□ for pristine and after plasma treatment for 20 s, respectively, whereas the R_{sh} values obtained from short channel TLM device are 0.67 and 3.13 kΩ/□. It should be noted that the obtained R_{sh} of short channel devices are quite similar with measured R_{sh} of graphene without device fabrication process. This manifests that the graphene channel region could be seriously affected by plasma even though it is protected by PMMA.

The scaling effects of plasma treatment are more clearly seen in the transfer curves as shown in Fig. 4(a) and (b). Fig. 4(a) shows the I_d vs V_g-V_{Dirac} curve obtained from the long channel device with L = 20 μm, V_d = 10 mV and V_g = –78 to +11 V. As shown in (a), Ar 20 s plasma treatment enhanced overall current. The value increased from 1.28 to 1.48 times when the V_g-V_{Dirac} varied from –80 to +20 V. The R_c

of the sample treated with the Ar plasma for 20 s was decreased in the entire V_g range. This may be attributed to the effect of sp^3 bonding, dangling bonds and vacancies induced by the plasma. Thus, the electric performance of the devices was improved due to the reduced R_c. Fig. 4(b) shows the I_d vs $V_g - V_{Dirac}$ curve obtained from the short channel device with $L = 375$ and 440 nm, $V_d = 10$ mV and $V_g - V_{Dirac} = -80$ to +10 V. As shown in (b), I_d was decreased after plasma treatment. This behavior is totally opposite to that for long channel devices. As we mentioned previously, the damaged region could decrease I_d significantly despite slightly reduced R_c. In order to interpret this phenomenon and estimate the damaged region, we drew schematic and circuit diagrams for the long and short channel devices as shown in Fig. 4(c). It is expected that there are three resistances; resistance of damaged region, contact resistance and channel resistance. For the long channel devices, the damaged region is quite shorter than total channel length. Thus, this region could be neglected and results in unchanged R_{sh}. The carriers probably tend to just tunnel through this region. In contrast, it cannot be ignored for the short channel devices. By calculating series resistance equation, a damaged region was estimated to be ~ 171 nm for 440 nm device. The ratio of damaged region to total channel length for long channel device is just 1.7 %, while 78 % for short channel device. As a result, the damaged area in the channel region can give rise to the significantly increased resistance resulting in decreased I_d for the short channel devices. Therefore, it is required to find the tradeoff point between R_c and L for plasma treated devices.

3. Conclusion

In this paper, the low power Ar plasma treatment method was studied to improve electrical performances in terms of R_c and R_{sh} of the graphene device with various channel lengths. The result shows R_c decreased more than 2 times by the 20 s Ar plasma treatment for the long channel devices. Thus, the current transport was enhanced by decreasing R_c when the proper Ar plasma treatment was performed. But the I_d decreased for short channel devices because of the dominance of the increased resistance at the physically bombarded edge of the channel, induced by Ar plasma treatment at the contact region. The proposed Ar plasma treatment is expected to be an effective method to minimize contact resistance of graphene based devices, as it is compatible to current low temperature and large scale electronic device fabrication processing.

Acknowledgements

This work was supported by the Global Frontier R&D Program (2013M3A6B1078873) at the Center for Hybrid Interface Materials (HIM), funded by the Ministry of Science, ICT & Future Planning.

References

[1] K. I. Bolotin, K. J. Sikes, Z. Jiang, M. Klima, G. Fudenberg, J. Hone, P. Kim, H. L. Stormer, Ultrahigh electron mobility in suspended graphene, Solid State Commun., 146 (2008) 351-355.

[2] J. H. Seol, I. Jo, A. L. Moore, L. Lindsay, Z. H. Aitken, M. T. Pettes, X. Li, Z. Yao, R. Huang, D. Broido, Two Dimensional Phonon Transport in Supported Graphene, Science, 328 (2010) 213-216.

[3] K. N. Parrish, D. Akinwande, Impact of contact resistance on the transconductance and linearity of graphene transistors, Appl. Phys. Lett., 98 (2011) 183505.

[4] J. A. Robinson, M. LaBella, M. Zhu, M. Hollander, R. Kasarda, Z. Hughes, K. Trumbull, R.Cavalero, D. Snyder, Contacting graphene, Appl. Phys. Lett., 98 (2011) 053103.

[5] W. Liu, J. Wei, X. Sun, H. Yu, A study on graphene—metal contact, Crystals, 3 (2013) 257-274.

[6] A. Hsu, H. Wang, K. K. Kim, J. Kong, T. Palacios, Impact of Graphene Interface Quality on Contact Resistance and RF Device Performance, IEEE Electron Device Lett., 32 (2011) 8, 1008-1010.

[7] W. Li, Y. Liang, D. Yu, L. Peng, K. P. Pernstich, T. Shen, A. R. Hight Walker, G. Cheng, C. A. Hacker, C. A. Richter, Q. Li, D. J. Gundlach, X. Liang, Ultraviolet/ozone treatment to reduce metal-graphene contact resistance, Appl. Phys. Lett., 102 (2013) 1831110.

[8] W. Chen, C. Ren, F. Chi, G.-C. Hung, S.-C. Huang, Y. P. Kim, J. Kravchenko, S. J. Pearton, UV ozone treatment for improving contact resistance on graphene, J. Vac. Sci. Technol. B., 30 (2012) 060604.

[9] Y. D. Lim, D.Y. Lee, T.Z. Shen, C.H. Ra, J.Y. Choi, W. J. Yoo, Si-compatible cleaning process for graphene using low-density inductively coupled plasma, ACS Nano, 6 (2012) 4410-4417.

[10] M. S. Choi, S. H. Lee, W. J. Yoo, Plasma treatments to improve metal contacts in graphene field effect

transistor, J. Appl. Phys., 110 (2011) 073305.
[11] S. Gahng, C. H. Ra, Y. J. Cho, J. A. Kim, T. Kim, W. J. Yoo, Reduction of metal contact resistance of graphene devices via CO2 cluster cleaning, Appl. Phys. Lett., 104 (2014) 223110.
[12] C. Gong, S. McDonnell, X. Qin, A. Azcatl, H. Dong, Y. J. Chabal, Kyeongjae Cho, R. M. Wallace, Realistic metal-graphene contact structures, ACS Nano, 8 (2014) 642-649.
[13] D. W. Yue, C. H. Ra, X. C. Liu, D. Y. Lee, W. J. Yoo, Edge contacts of graphene formed by using a controlled plasma treatment, Nanoscale, 7 (2015) 825-831.
[14] K. Nagashio, T. Nishimura, K. Kita, A. Toriumi, Metal/Graphene Contact as a Performance Killer of Ultra-high Mobility Graphene - Analysis of Intrinsic Mobility and Contact Resistance , IEEE International Electron Devices Meeting, (2009) 565-568.
[15] K. Nagashio, T. Nishimura, K. Kita, A. Toriumi, Contact resistivity and current flow path at metal/graphene contact, Appl. Phys. Lett., 97 (2010) 143514.
[16] K. Nagashio, A. Toriumi, DOS-limited contact resistance in graphene FETs, Jpn. J. Appl. Phys., 50 (2011) 070108.
[17] F. Xia, V. Perebeinos, Yu-ming Lin, Y. Wu, P. Avouris, The origins and limits of metal-graphene junction resistance, Nat. Nanotech., 6 (2011) 179-184.
[18] F. Ahmed, M. S. Choi, X. Liu, W. J. Yoo, Carrier transport at the metal–MoS 2 interface, Nanoscale, 7 (2015) 9222-9228.
[19] A. D. Franklin, S.-J. Han, A. A. Bol, V. Perebeinos, Double Contacts for Improved Performance of Graphene Transistors, IEEE Electron Device Lett., 33 2012) 17-19.
[20] Y. Matsuda, W.-Q. Deng, W. A. Goddard III, Contact Resistance for “End-Contacted” Metal−Graphene and Metal−Nanotube Interfaces from Quantum Mechanics, J. Phys. Chem C, 114 (2010) 17845-17850.
[21] J. T. Smith, A. D. Franklin, D. B. Farmer, C. D. Dimitrakopoulos, Reducing contact resistance in graphene devices through contact area patterning, ACS Nano, 7 (2013) 3661-3667.
[22] L. Wang, I. Meric, P. Y. Huang, Q. Gao, Y. Gao, H. Tran, T. Taniguchi, K. Watanabe, L. M. Campos, D. A. Muller, J. Guo, P. Kim, J. Hone, K. L. Shepard, C. R. Dean, One-dimensional electrical contact to a two-dimensional material, Science, 342 (2013) 614-617.
[23] W. S. Leong, H. Gong, J. T. L. Thong., Low-contact-resistance graphene devices with nickel-etched-graphene contacts, ACS Nano, 8 (2014) 994-1001.
[24] J. Chen, T. Shi, T. Cai, T. Xu, L. Sun, X. Wu, D. Yu, Self healing of defected graphene, Appl. Phys. Lett., 102 (2013) 103107.
[25] X. Lia, W. Caia, J. Ana, S. Kimb, J. Nahb, D. Yanga, R. Pinera, A. Velamakannia, I. Junga, E. Tutucb, S. K. Banerjeeb, L. Colombo, R. S. Ruoff, Large-area synthesis of high-quality and uniform graphene films on copper foils, Science, 324 (2009) 1312-1314.
[26] X. Li, W. Cai, L. Colombo, R. S. Ruoff, Evolution of graphene growth on Ni and Cu by carbon isotope labeling, Nano Lett., 9 (2009) 4268-4272.
[27] L. G. Cancado, A. Jorio, E. H. M. Ferreira, F. Stavale, C. A. Achete, R. B. Capaz, M. V. O. Moutinho, A. Lombardo, T. S. Kulmala, A. C. Ferrari, Quantifying Defects in Graphene via Raman Spectroscopy at Different Excitation Energies, Nano Lett., 2011, 11, 3190-3196.
[28] A. C. Ferrari, Raman spectroscopy of graphene and graphite: Disorder, electron–phonon coupling, doping and nonadiabatic effects, Solid State Commun., 143 (2007) 47-57.
[29] P. Venezuela, M. Lazzeri, F. Mauri, Theory of double-resonant Raman spectra in graphene: Intensity and line shape of defect-induced and two-phonon bands, Phys. Rev. B, 84 (2011) 035433.
[30] A. Eckmann, A. Felten, A. Mishchenko, L. Britnell, R. Krupke, K. S., Novoselov and C. Casiraghi, Probing the Nature of Defects in Graphene by Raman Spectroscopy, Nano Lett., 12 (2012) 3925-3930.
[31] S. S. Cohen, Contact Resistance and Methods for Its Determination, Thin Solid Films, 104 (1983) 361-379.
[32] W. M. Loh, S. E. Swirhun, T. A. Schreyer, R. M. Swanson, K. C. Saraswat, Modeling and measurement of contact resistances, IEEE Trans. Electron Devices, 34 (1987) 512-524.
[33] D. K. Schroder, Semiconductor material and device characterization, 3rd ed. Wiley, New York, (2006) 147.